



## DIRECT THERMOELECTRIC MICROGENERATION USING RESIDUAL HEAT OF PHOTOVOLTAIC SYSTEM<sup>1</sup>

José Rui Camargo | rui@unitau.br | UNITAU

Jalmir Machado Silva | jalmir.machado@gmail.com | UNITAU

Ederaldo Godoy Junior | godoyjr@unitau.br | UNITAU

### ABSTRACT

All photovoltaic panel heats up when exposed to sunlight and this heating reduces the electrical power output of the same. This work presents the use of this unwanted waste heat, converting it into thermal energy directly by means of the Seebeck effect, which is the direct conversion of thermal energy into electrical energy by means of an arrangement of semiconductor materials that when exposed to temperature gradients generate electric current. In this work emphasis was placed on the influence of temperature on generation processes involved. Thus, the theoretical evaluation, it presents the mathematical models of thermoelectric and photovoltaic systems by raising the curves of voltage, current and electric power generated, and analyses the influence of temperature in each model. To obtain the simulation curves it uses MATLAB<sup>®</sup> 5.3, taking into account the parameters of thermoelectric modules and real photovoltaic cells. In practical evaluation, a prototype was assembled containing thermoelectric module attached to the bottom of a photovoltaic panel in order to use the heat energy absorbed by the panel. The data were stored and analyzed, where we observed the influence of temperature in both systems, validating the mathematical modeling. It is the applicability of the mathematical model given the results obtained with the prototype system.

**Keywords:** Photovoltaic effect, Seebeck effect, Direct termoelectricity.

### INTRODUCTION

The growing environmental concern, the quest for increased association of clean and sustainable energy alternatives, such as photovoltaics and thermoelectric direct.

The cost of photovoltaic cells is a major challenge for the industry and the main obstacle to the spread and consolidation of large-scale systems. With the current environmental problems, the cost of photovoltaic solar energy has become in some countries more attractive than the cost of traditional energy sources; this is because parameters such as pollution of air and water that were not taken into account in the past are increasingly longer present.

---

1 Artigo publicado nos Anais do Congresso Microgen 2013

The thermoelectric power is obtained in the direct conversion of heat into electricity (Seebeck effect). The phenomenon is the development of a potential difference between two conductive or semiconductor junctions composed of different materials, when they are at different temperatures.

The thermoelectric power has been out of scientific focus for years, it was initially used only with metal conductors in order to measure temperature, but with the discovery of semiconductors, thermoelectric began to be studied with the purpose of power generation. One of the great difficulties of the system is to develop materials that provide better performance. Currently, the thermoelectric power has applications in some areas like power generation for control systems, military communications, aerospace, power generation for remote monitoring stations in areas of oil exploration.

The objective of this work is the development of a prototype system composed of a thermoelectric module coupled to a photovoltaic panel to take advantage of residual heat from the panel. In this case, the thermoelectric module has its hot side in contact with the lower surface of the photovoltaic panel which is heated by exposure to solar radiation, to provide an electric power generation by the thermoelectric module through the Seebeck effect.

Are presented mathematical models of the photovoltaic and thermoelectric and the results obtained after trials conducted with a prototype system for recovery of residual heat from the photovoltaic generation process.

**Direct Thermoelectric Module.** Generally more than one pair of semiconductors are mounted together to compose a thermoelectric device (module) and inside the module, each of the semiconductors is called a thermo element.

To describe the operation of thermoelectric modules can compare them with the thermocouples. Thermocouples are devices that generate a potential difference (DDP) from the two junctions of different metals which are at different temperatures and are used to indicate and control the temperature in many industrial processes.

A thermoelectric device typically comprises two carcasses ceramics, which serve as a frame to preserve the mechanical integrity of the module and how electrical isolation for the thermoelements bismuth telluride n-type and p-type, which are electrically connected in series and thermally in

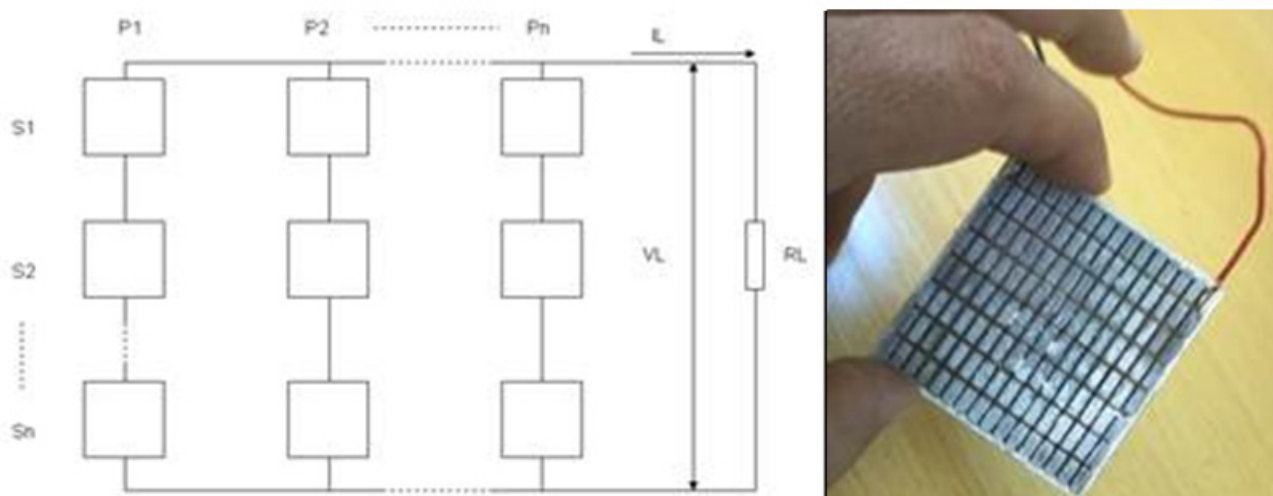
parallel between the ceramic plates. The devices usually contain 3-127 thermocouples. Copper is used as electrical conductive material between the semiconductor posted in parallel. The system is connected by welding.

The application module for power generation requires a higher compression of the thermocouples in the case of generation or heat absorption (Alves, 2007).

In applications where one requires increased power supplied by the source, only one module does not supply the necessary energy to the load.

Thus, should be used in the module series arrangements, for raising the voltage level output, and in parallel to increase the level of output current, or even the arrangement series / parallel both to raise the voltage level as required by the load current. Figure 1 illustrates an arrangement of thermoelectric modules and a view emphasizing the arrangement.

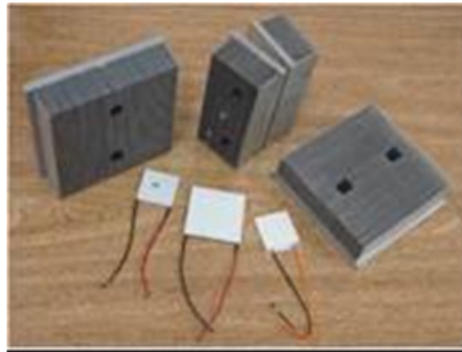
**Figure 1 - Arrangement of thermoelectric modules and a view emphasizing the arrangement of module open.**



An element essential for the proper functioning of the thermoelectric module for power generation is the proper use of the heat sink. This is in direct contact with the cold side of the module, you must have a minimum thermal resistance between them. The objective is to remove heat sink of the cold side of the plate to maintain the temperature as low as possible. A heat sink would be perfectly capable of absorbing an unlimited amount of heat without showing any temperature increase. Since this is not possible in practice, was selected a heat sink, with an acceptable temperature rise during

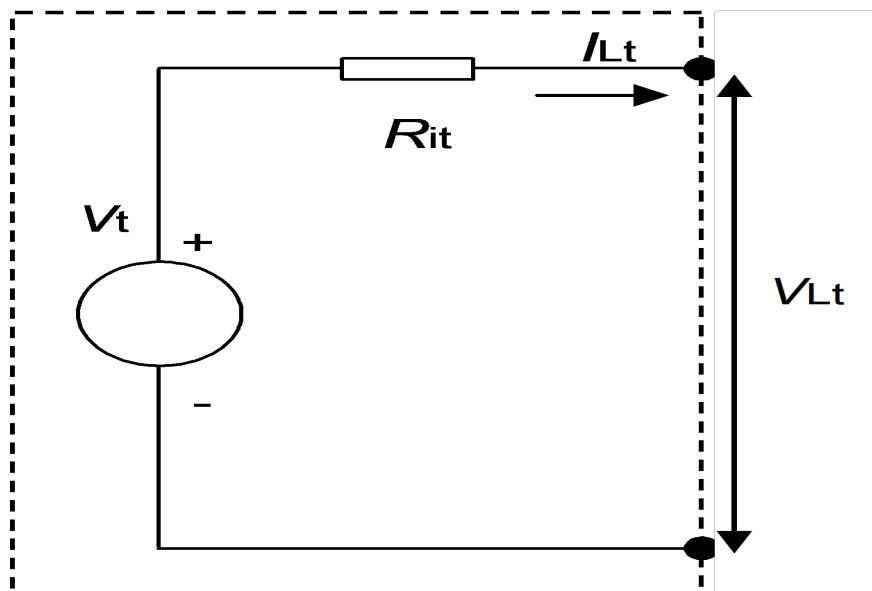
operation of the thermoelectric module. To avoid the negative effect of the heat sink, it is desirable that its temperature is at most 5 °C above room temperature (Spencer, 2007). Various types of heat sinks are available, including natural convection, forced convection, and liquid cooling. This research used sinks natural convection. Figure 2 illustrates the heat sinks and natural convection thermoelectric modules used.

**Figure 2** - Thermoelectric modules and heat sinks (CAMARGO et al, 2008)



**Mathematical Model of a thermoelectric module.** Figure 3 illustrates the module provided without load connected to its output terminals.

**Figure 3** - Simplified model thermoelectric module unloaded.



Based on the Seebeck effect, is that the open circuit voltage is given by Equations (1) to (4).

$$V_t = \alpha \Delta t \tag{1}$$

$$V_{Lt} = V_t \tag{2}$$

Where:

$$\Delta t = t_2 - t_1 \quad (3)$$

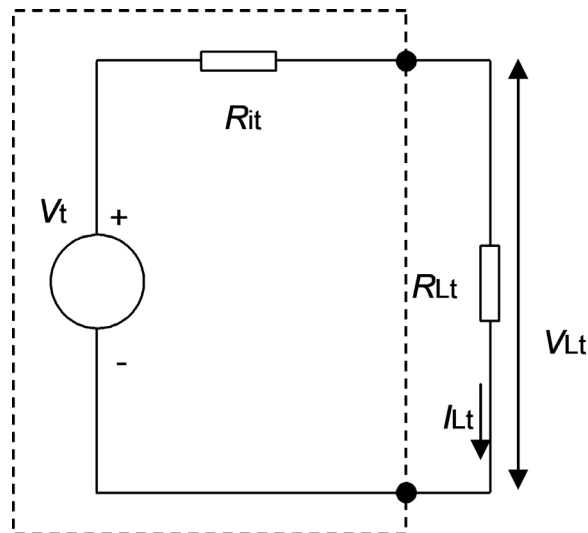
$$\alpha = \alpha_1 + \alpha_2 \quad (4)$$

are the parameters and material properties of the circuit and are electromotive forces appearing in the materials 1 and 2 due to temperature difference of 1° C between the ends. Thus, substituting Equations (3) and (4) in Equation (1), the potential difference is given by Equation (5).

$$V_t = (\alpha_1 + \alpha_2) \times (t_2 - t_1) \quad (5)$$

As the circuit is open, as shown in Figure 3, there is no electric current. When connecting a load resistor, as shown in Figure 4, the terminals of the module appear an electric current.

**Figure 4 - Model of a thermoelectric module with load**



The load current is given by Equation (6). The load voltage is given by Equation (7).

$$I_{Lt} = \frac{V_t}{(R_{it} + R_{Lt})} \quad (6)$$

$$V_{Lt} = I_{Lt} R_{Lt} \quad (7)$$

The power generated in the load is given by Equation (8).

$$P_{Lt} = V_{Lt} I_{Lt} \quad (8)$$

Substituting Equations (6) and (7) in Equation (8) has Equation (9).

$$P_{Lt} = \frac{V_t^2 R_{Lt}}{(R_{it} + R_{Lt})^2} \quad (9)$$

Substituting Equations (3) and (4) in Equation (9) has Equation (10) the power produced in the circuit.

$$P_{Lt} = (\alpha_1 + \alpha_2)^2 (t_{2t} - t_{1t})^2 \frac{R_{Lt}}{(R_{it} + R_{Lt})^2} \quad (10)$$

To set the value of load resistance that will allow the system operates at its maximum. The point where the power is maximum is where power is derived from the load resistance equal to zero.

Thus for maximum power, should be equal to the load resistance internal resistance of the thermoelectric module. This will be the resistance value to maximize power at the load.

$$\frac{V_t^2 (R_{it} + R_{Lt}) - 2 R_{Lt} V_t^2}{(R_{it} + R_{Lt})^2} = 0 \Rightarrow V_t^2 (R_{it} + R_{Lt}) = 2 R_{Lt} V_t^2 \Rightarrow (R_{it} + R_{Lt}) = 2 R_{Lt} \Rightarrow R_{Lt} = R_{it} = R_{\text{maxpot}} \quad (11)$$

Substituting Equation (11) in Equation (9) has to Equation (12) representing the maximum power in the load.

$$P_{\text{max}} = (\alpha_1 + \alpha_2)^2 (t_{2t} - t_{1t})^2 \frac{R_{\text{maxpot}}}{(R_{\text{maxpot}} + R_{\text{maxpot}})^2} \Rightarrow P_{\text{max}} = \frac{(\alpha_1 + \alpha_2)^2 (t_{2t} - t_{1t})^2}{4 R_{\text{maxpot}}} \quad (12)$$

## METHODOLOGY

The methods used for this work are simulations and tests with thermoelectric and photovoltaic systems based on the theories presented.

**Simulations.** For the simulations of the mathematical models presented in the study, was used the software MATLAB<sup>®</sup> 5.3, which is a high performance software designed to do calculations with matrices (MATrix LABoratory) and may act as a calculator or as a scientific programming language (FORTRAN, Pascal, C, etc.). However, the MATLAB commands are closer to the way we write algebraic expressions, making it easier to use. MATLAB is defined as an interactive system and programming language for scientific and technical computing in general, integrating the ability to

make calculations, graphical visualization and programming (Tonini and Schettino 2002).

For the implementation of mathematical models in MATLAB<sup>®</sup> 5.3, codes were created. Table 1 shows the description of each code. For the photovoltaic cells and the thermoelectric modules were simulated curve of current, voltage and power in the load to generate information for analysis.

**Table 1 - Description of the codes**

Code	Description
A	Simulation of a photovoltaic cell at a temperature of 25° C
B	Simulation of a photovoltaic cell at a temperature of 50° C
C	Simulation of a photovoltaic cell at a temperature of 75° C
D	Simulation of a photovoltaic cell at a temperature of 25° C, 50° C e 75° C
E	Simulation of a thermoelectric module with a variation of load resistance from 0 to 35 Ω
F	Simulation of a thermoelectric module with a change in the warm side temperature of 30° C to 80° C
G	Simulation of a thermoelectric module with a change in the warm side temperature of 80°C to 30°C
H	Comparative analysis of the simulated model and the data measured on a photovoltaic prototype to a temperature of from the 54° C
I	Comparative analysis between the model simulated and measured data in the prototype for a thermoelectric system

**Photovoltaic System.** The theoretical model presented was simulated in MATLAB<sup>®</sup> 5.3, thus obtaining the system's behavior by temperature variations. For purposes of analysis were considered typical parameters supplied by the manufacturer of photovoltaic modules. Where:  $V_{caf} = 20V$ ;  $I_{ccf} = 0,7A$ ;  $P_{Lmaxf} = 10W$ ;  $I_{Lmaxf} = 0,6A$ ;  $V_{Lmaxf} = 16,5V$ ;  $e_{ncs} = 36$

The terms of reference standard for testing photovoltaic modules are entitled as a condition standard for testing and is set to the incident radiation ( $Gr=1000 W/m^2$ ), and temperature ( $tr=25° C$ )

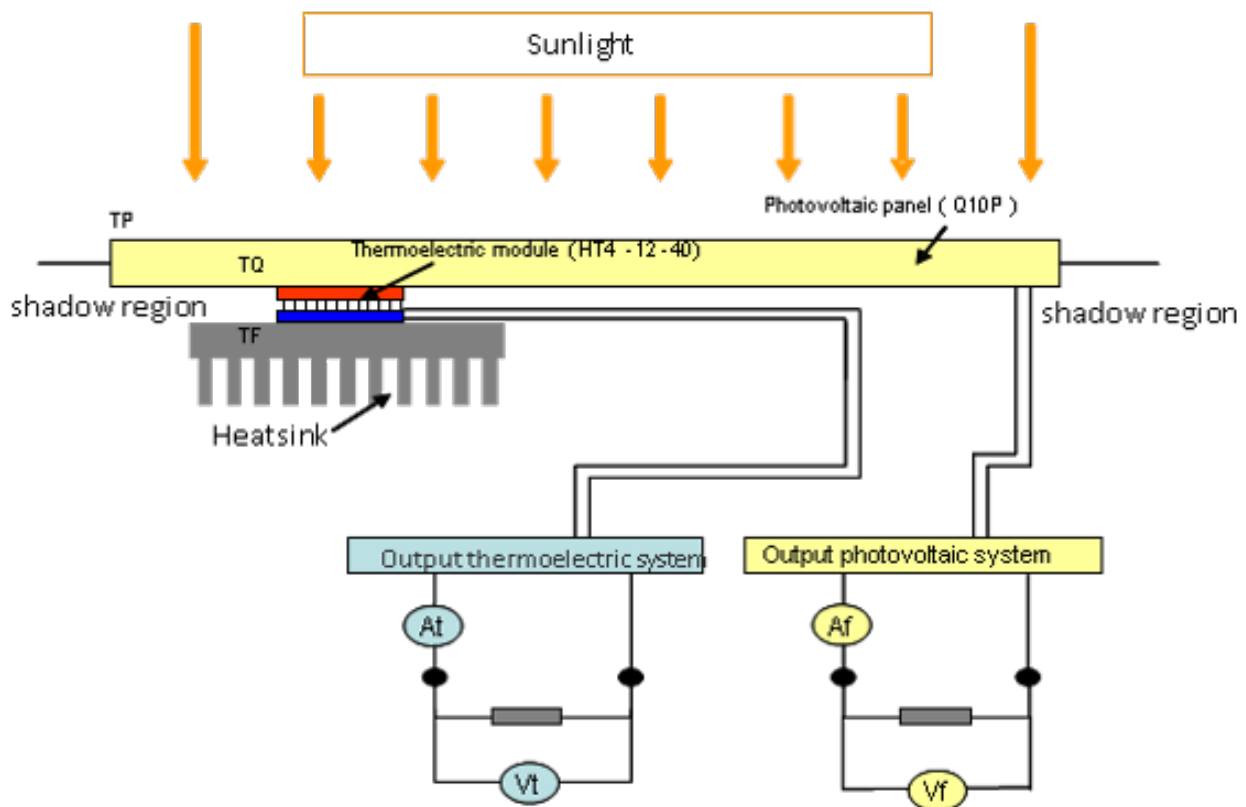
**Thermoelectric System.** The theoretical model presented was simulated in MATLAB<sup>®</sup> 5.3, thus obtaining the system's behavior. Were considered typical parameters that are provided by the manufacturer. Which are:  $R_{it} = 3,49 \Omega$ ;  $\alpha = 0,053 V/K$ , from the manufacturer's specification sheet, can be determined using Equation (1), the Seebeck coefficient in the same.

**Experimental System.** For the practical study of the presented system, an experimental prototype was assembled to observe the generation of electricity. The system is composed of photovoltaic panel: Conergy Manufacturer: Model: Q 10P; Thermoelectric module: Manufacturer:

Melcor, Model: HT 4-12-40, heat sink - Employee on the cold side, aluminum, measuring 154 x 80 x 40 mm, fins 38 and fins spacing of 2 mm, thermo-hygrometer for measuring temperature; multimeters "Minipa ET-1001", for measuring current and voltage; stock resistors 2.5  $\Omega$  at 1500  $\Omega$ .

Although the thermoelectric module model HT4-12-40 manufacturer Melcor be aimed at cooling the same experiment in this study was used to generate electricity, thus proving the inversion between the Peltier and Seebeck effects. The collected data were entered into the spreadsheet software Microsoft Office Excel 2003®, to generate tables and graphs to optimize the analysis.

Figure 6 illustrates a proposed scheme for the prototype system. At the bottom of the photovoltaic panel, coupled to the thermoelectric module so that the hot side stay in direct contact with the panel, since the cold side in contact with the heatsink in the shade.



For measurement and subsequent evaluation of the variables involved in the process illustrated in Figure 6 we have: the first thermo-hygrometer for measuring surface temperature of the solar panel (TP), the second thermo-hygrometer for measuring the warm side of the thermoelectric module (TQ), the third thermo-hygrometer to measure temperature of the cold side of thermoelectric

plate (TF), the first ammeter for measuring electrical current output of the thermoelectric system (At), the second ammeter for measuring electrical current output of the photovoltaic system (Af), the first voltmeter for measuring the voltage output thermoelectric system (Vt), and finally the second voltmeter for measuring voltage output of the photovoltaic system (Vf).

For evaluation of the assay was taken into consideration at room temperature (TA), the temperature of the solar panel (TP), the temperature of the hot side of the thermoelectric module (TQ), the temperature of the cold side of the thermoelectric module (TF), the current generated by photovoltaic (Af), the tension generated by the photovoltaic system (Vf), the current generated by the thermoelectric system (At) and the tension generated by the thermoelectric system (Vt).

The system was exposed to sunlight and measurements needed to evaluate the system were taken. For a better quality of analysis, measurements of photovoltaic and thermoelectric were collected at the same time.

The characteristics of accuracy of measuring instruments are presented in Table 2.

**Table 2 - Characteristics of measuring instruments**

Instrument	Model	Resolution/Tolerance
Termo-higrometer	Politerm	1°C / ± 0,05 %
Multimeter	Minipa/ET 1001	0,005V / ± 0,5%
Multimeter	Minipa/ET 1001	0,05A / ± 1%

Measurements were made on clear days in the period between twelve hours and fourteen hours.

Two experiments were conducted on different days, because after the first test was detected problems in the thermoelectric system that was necessary to treat and then retested.

After treatment of the problem encountered, the system was again tested.

In Figure 7 (a) illustrates the bank of resistors, and multimeters termo-higrometers for measuring variables involved, and (b) illustrates the photovoltaic panels exposed to solar radiation, and the power cables and load measuring devices directed for an internal point of the building's shadow.

Only it was considered the measurement referring to the panel that is installed with the thermoelectric module.

**Figure 7 -** Measuring and stock at the internal resistance (a) and the external part (b) the photovoltaic panels exposed to solar radiation

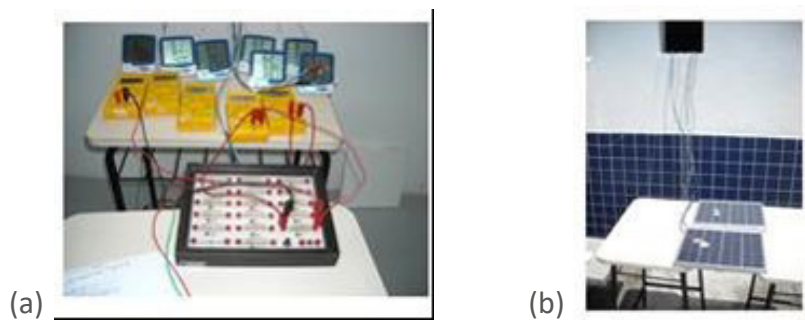


Figure 8 illustrates heat sink which is connected to the cold side of the thermoelectric module, which in turn has its hot side connected to the bottom of the photovoltaic panel. The panel acts as the propagation of heat to the hot side of the thermoelectric module. Power cables and measurement are forwarded to an internal point of the building's shadow.

**Figure 8 -** Heat sink and thermoelectric module connected to the photovoltaic panel.



Figure 9 illustrates the improvement made after problems encountered during the first measurement, where the thermal insulation applied polyurethane around the thermoelectric modules. For these measurements was considered only one thermoelectric module.

**Figure 9 -** Set sink, thermoelectric modules and photovoltaic panel with installation of thermal insulation.



## COMPARISON BETWEEN SIMULATIONS AND TESTING

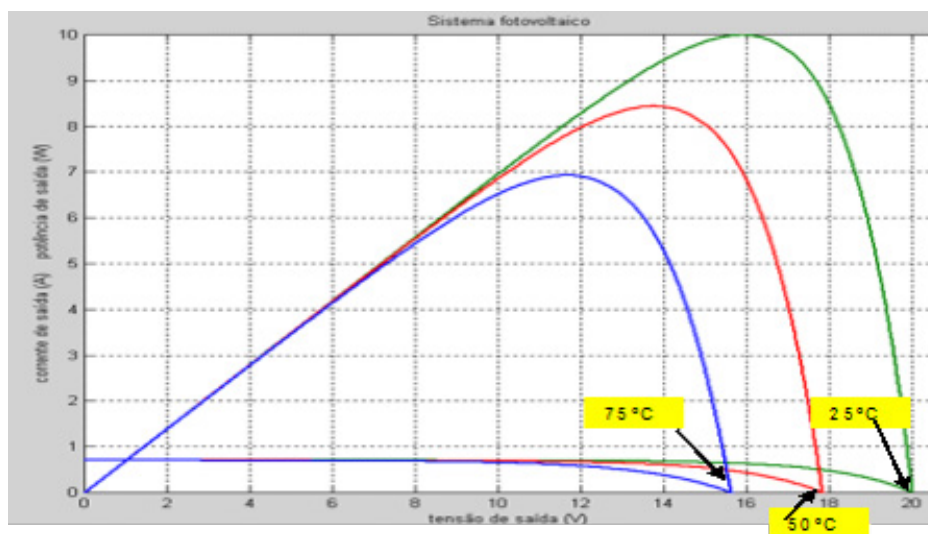
In order to graphically compare the results of mathematical models for some generated graphs and data obtained during the tests, was created in MATLAB<sup>®</sup> 5.3 code, simulating the same graph, the theoretical data based on mathematical models and practical data collected during the tests.

## RESULTS AND DISCUSSION ARISING FROM SIMULATIONS AND MEASUREMENTS PERFORMED IN COLLECTED AND EXPERIMENTAL SYSTEM

**Simulations of the Photovoltaic System.** The mathematical model developed for the photovoltaic system was used for the creation of codes for the simulation in MATLAB<sup>®</sup> 5.3.

Figure 10 illustrates the simulation of a photovoltaic module in all three cases, in other words, photovoltaic modules at temperatures 25° C, 50° C and 75o C. Is clearly observed the influence of temperature of the photovoltaic cells to generate electricity. The increase in temperature reduces the generated voltage in the load ( $V_{Lf}$ ) and consequently the power ( $P_{Lf}$ ) has its value reduced.

**Figure 10 - Curves ( $I_{Lf} \times V_{Lf}$  e  $P_{Lf} \times V_{Lf}$ ) at temperatures of 25°C, 50°C e 75°C**



Thermoelectric System. The mathematical model developed for the thermoelectric system was used for the creation of codes for the simulation in MATLAB<sup>®</sup> 5.3.

Figure 11 illustrates the simulation of the thermoelectric module, showing the curves of the load voltage ( $V_{Lt}$ ), power load ( $P_{Lt}$ ) and load current ( $I_{Lt}$ ) X load resistance ( $R_{Lt}$ ). It is observed with increasing value of load resistance, high output voltage and reducing the output current, since power value has increased to the point of maximum power ( $P_{max}$ ), as shown in the mathematical

model. The maximum occurs when the load resistance ( $R_{Lt}$ ) equals the value of internal resistance of the module ( $R_{it}$ ), after this value is observed a reduction in output power. For the simulation was considered the amount of  $3,49\Omega$  to the internal resistance of the module, so the maximum power point occurs when the load resistance is equal to  $3,49\Omega$ .

**Figure 11** - Curves (V<sub>Lt</sub>, P<sub>Lt</sub>, I<sub>Lt</sub> X R<sub>Lt</sub>) for a variation of load resistance 0  $\Omega$  at 35 $\Omega$

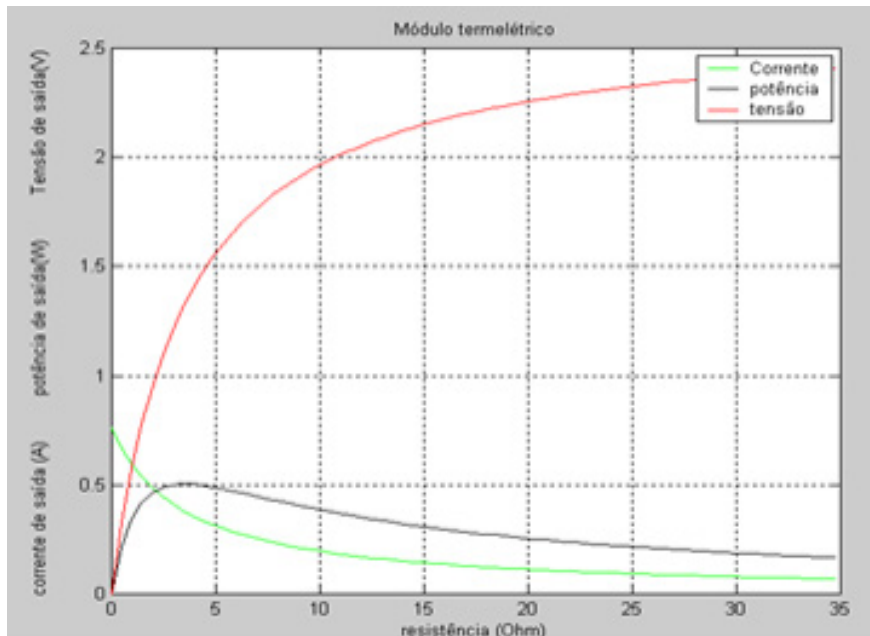
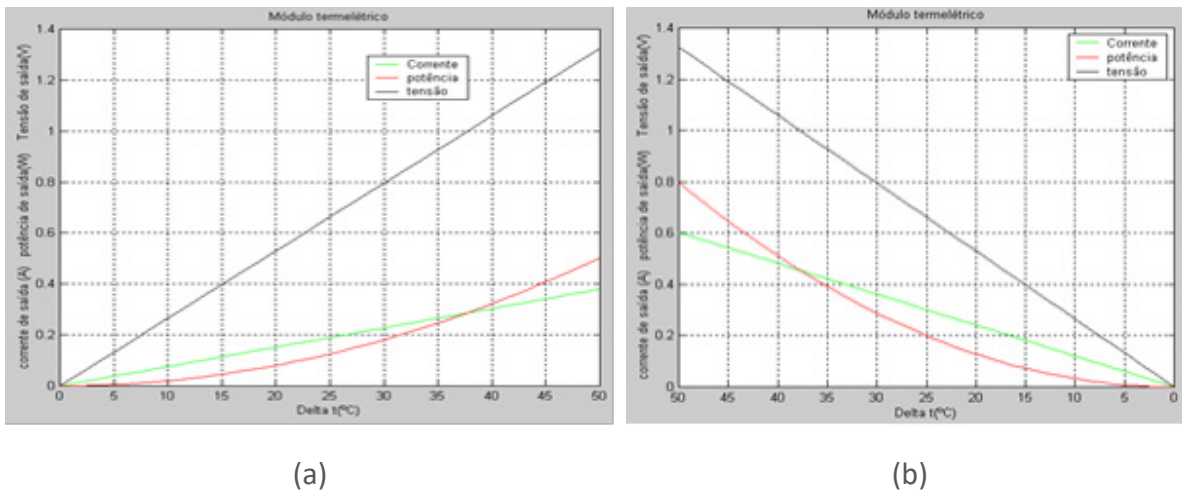


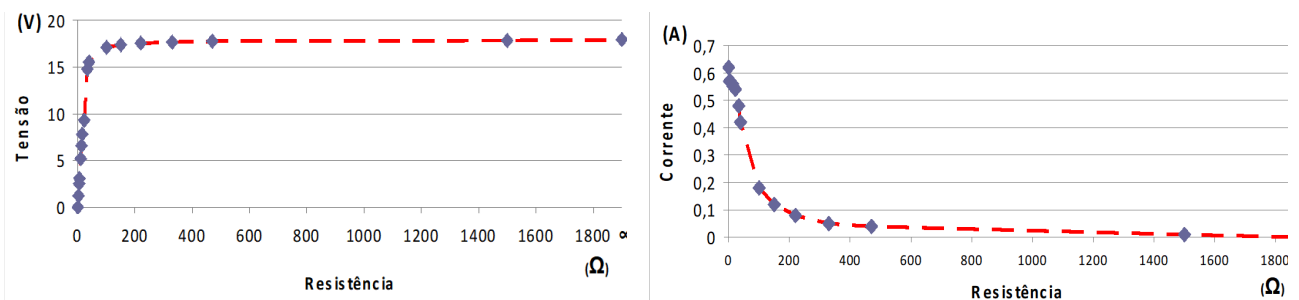
Figure 12 illustrates the simulation of the thermoelectric module, showing the curves of the load voltage (V<sub>Lt</sub>), power load (P<sub>Lt</sub>) and load current (I<sub>Lt</sub>) X  $\Delta t_t$  (the hot side temperature minus the temperature of the cold side). It was considered an elevated temperature on the hot side of the 80o C to 30° C with a constant temperature on the cold side and equal to 30° C. It is observed with increasing amount of  $\Delta t_t$ , High levels of voltage, current and power in charge. From Figure 16 the graph of the simulation of thermoelectric module, showing the curves of the load voltage (V<sub>Lt</sub>), power load (P<sub>Lt</sub>) and load current (I<sub>Lt</sub>) X  $\Delta t_t$  (the hot side temperature minus the temperature of the cold side). It was considered a reduction in temperature on the hot side of 80° C to 30° C with a constant temperature on the cold side equal to 30o C. It was observed by reducing the value of  $\Delta t_t$ , reducing the levels of voltage, current and power in the load. The behavior in the Graph (a) is the inverse to that shown in Graph (b) of Figure 12.

**Figure 12 - Curves (V<sub>Lt</sub>, P<sub>Lt</sub>, I<sub>Lt</sub> X Δt<sub>t</sub>) to a Δt<sub>t</sub> of 0°C in a) 50°C and a Δt<sub>t</sub> of 50°C at 0°C in b)**



**First Experimental Test System Photovoltaic (measurement 1).** Figure 13 illustrates the behavior of the output voltage or the load when there is a change in load resistance. This was varied from 2.5 Ω and 1500 Ω, thereby graphically is possible to observe similar behavior to the short-circuit voltage to the resistance value of 2.5 Ω or 0V and a tendency to open circuit voltage with the value of resistance of 1500 Ω. Also illustrated in Figure 13 is the behavior of the output current, when there is a change in load resistance. Was varied from 2.5 Ω and 1500 Ω, thereby graphically observed a similar behavior for the maximum current value of resistance of 2.5 Ω or 0.6 A and current behavior near open circuit to the resistance value 1500 Ω or 0 A.

**Figure 13 - Measurement 1 - X load resistor voltage photovoltaic module**



Equation (13), which describes the calculation of the power load may be interpreted as the product of the values of the graphs of Figures 18 and 19.

The power load for any point on the curve IV, is given by Equation (13).

$$P_{L_f} = V_{L_f} I_{L_f} \tag{13}$$

Figure 14 illustrates the behavior of the output power or load, when there is a change in load resistance. This was varied from 2.5 Ω and 1500 Ω, thereby graphically the behavior of the output power level has increased to reach a particular value of load resistance, the value is thereafter reduced.

The maximum power of the photovoltaic system,  $P_{Lmaxf}$ , according to Equation (14), is due to maximum stress (represented by  $V_{Lmaxf}$ ) and the maximum current (represented by  $I_{Lmaxf}$ ). By the law of Ohm, the load resistance that will promote the greatest power (Cabral, 2009):

$$R_{Lmaxf} = \left( \frac{V_{Lmaxf}}{I_{Lmaxf}} \right) \quad (14)$$

Analyzing the data supplied by the manufacturer, where  $V_{MPP}$  corresponds to  $V_{Lmaxf}$  and  $I_{MPP}$  corresponds to  $I_{Lmaxf}$ , and using the equation (14), has the value of  $R_{Lmaxf}$  equal to 27,5 Ω. Test performed by the resistance with the highest power value was equal to 33,2 Ω, close to the theoretical value. The power value is around 7 W, less than the value of 10W nominal for this module, in this way there is the influence of temperature behavior by making the mathematical model shown. As shown in Equation (13) of the mathematical model, one can see graphically a value of load resistance which is a maximum in its potency assay.

**Figure 14 - Measurement 1, X power load resistance to the photovoltaic module**

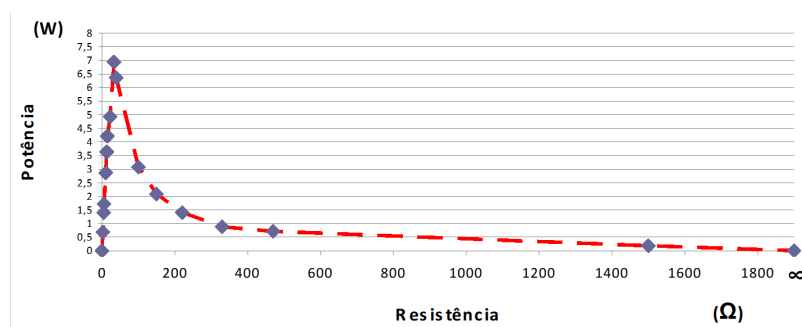


Figure 15 illustrates a graph of characteristic curves I - V of a photovoltaic module. The load resistance was 2.5 Ω range of 1500 Ω, and so the values measured voltage and load current.

It has been found to approximate the characteristic curve shown in theory, we observed the tension values of open circuit and short circuit current.

This curve follows Equation (15), the mathematical model of the PV system. Equation (15) is used to draw the characteristic curves I - V of the photovoltaic system.

**Figure 15 - Measurement 1, X current output voltage to the photovoltaic module**

$$I_{Lf} = I_{ccf} - I_o \left( e^{\frac{V_{Lf}}{mV_t}} - 1 \right) \quad (15)$$

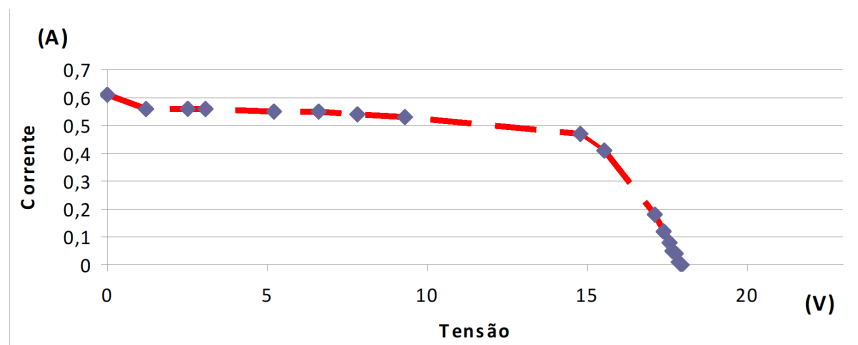


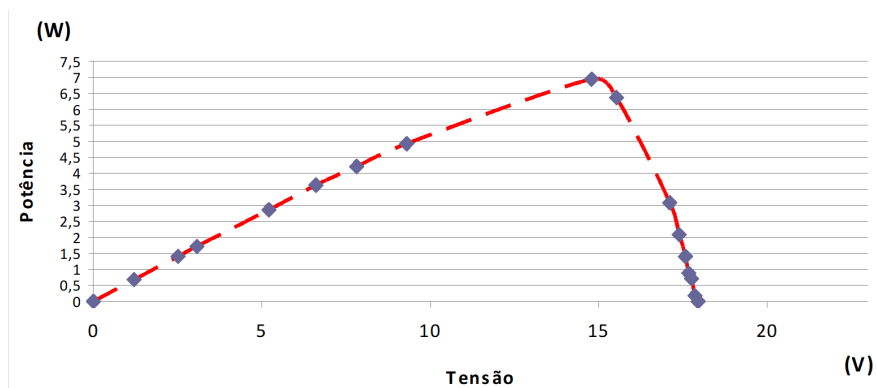
Figure 16 illustrates the graph of the characteristic curve Q - V of a photovoltaic module. The load resistance was 2.5 Ω range of 1500 Ω, and were thus measured values of voltage, current and load was calculated immediately after the power load.

There is the approximation of the characteristic curve shown in theory, you can see the value of maximum load or output. This curve follows Equation (16), presented the mathematical model.

Equation (16) is used to find the characteristic curve of PV.

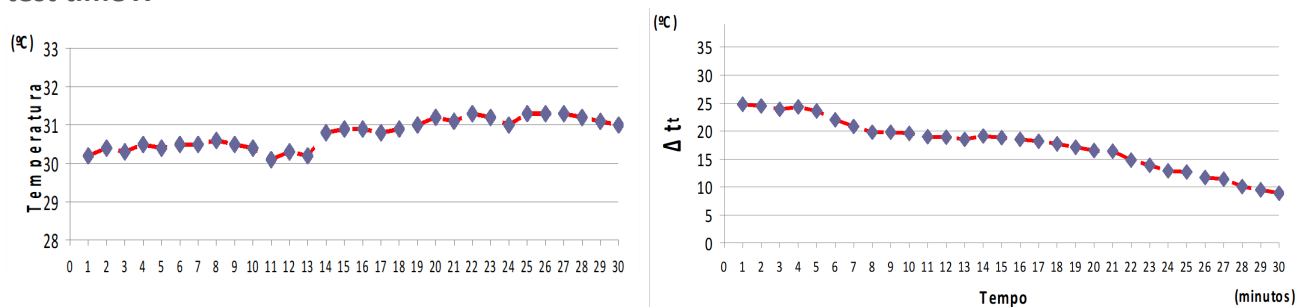
**Figure 16 - Measurement 1, X power load voltage for the PV module**

$$P_{Lf} = V_{Lf} \left\{ I_{ccf} - [I_o (e^{\frac{V_{Lf}}{mV_t}} - 1)] \right\} \quad (16)$$



**Thermoelectric System – measurement 1.** Figure 17 illustrates the behavior of the temperature for thirty minutes of the test system for the thermocouple. There is a slight increase of 1° C during the test period which is not represented problems.

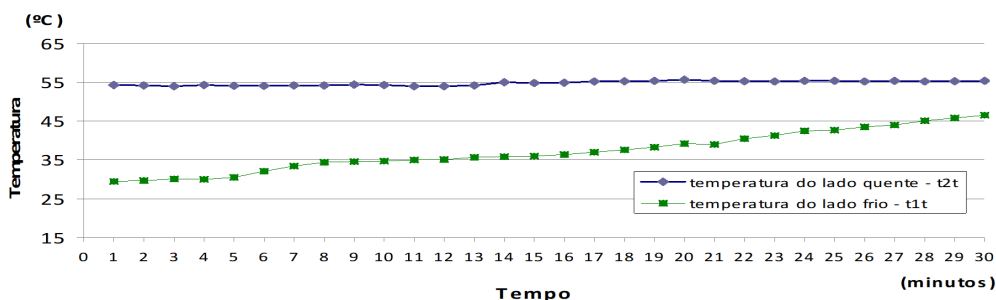
**Figure 17 - Graphs of the measurements 1, X temperature test time,  $\Delta T_t$  thermoelectric module test time X**



The chart of Figure 14 is shown the behavior of  $\Delta T_t$  thermoelectric module which is the difference between the temperature of the hot side and cold side at the time of test performed. There is a marked reduction in the amount of  $\Delta T_t$ . This fall marked a significant influence on reducing the level of electricity generation by thermoelectric module. Equation (3) brings the mathematical model calculation  $\Delta T_t$  showing its relationship between the temperature of the hot and cold sides of a thermoelectric module.

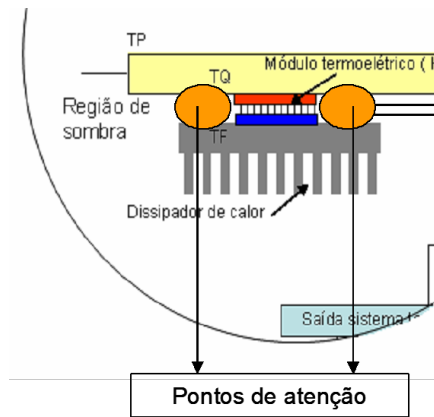
Figure 18 illustrates the behavior of the temperature of the hot side and cold side of the thermoelectric module. There is a slight increase of about 1° C in temperature of the hot side during the sampled period, already in the cold side there is a considerable elevation of temperature during the test, the first time the temperature is about 29.5° C and after thirty minutes it is already in the 46.5° C, an increase of about 17° C. This represents a technical obstacle to testing.

**Figure 18 - Measurement 1, temperature hot side and cold side test time X**



Looking at Figure 19, you can check some phenomena that influence the elevation of temperature of the cold side of thermoelectric module. The areas represent points where attention is possible to spread the heat of the hot side to cold side and the heatsink, so it is necessary to fill those areas with suitable insulating material, consisting of polyurethane, in order to minimize the temperature rise cold side and sink.

**Figure 19 - Analysis of the problem of heat propagation**



Consequently the reduction of  $\Delta T_t$ , Figure 20 illustrates the reduction of the output voltage. This proves the mathematical relationship found in Equation (1).

**Figure 20 - Measurement 1, the load voltage thermoelectric module X test time**

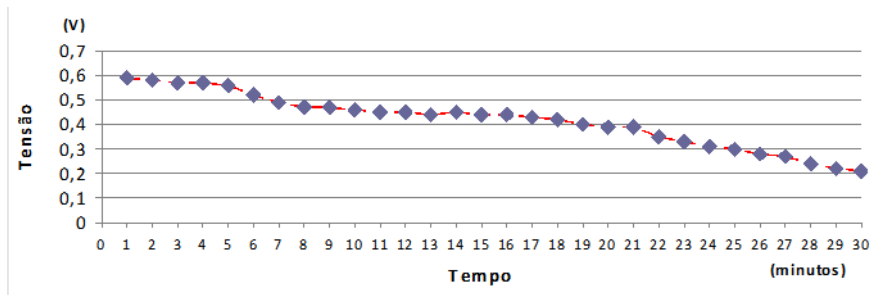


Figure 21 illustrates the reduction of the output current for a given load due to the reduction of  $\Delta T_t$  thermoelectric module.

**Figure 21 - Measurement 1, the load current thermoelectric module X test time**

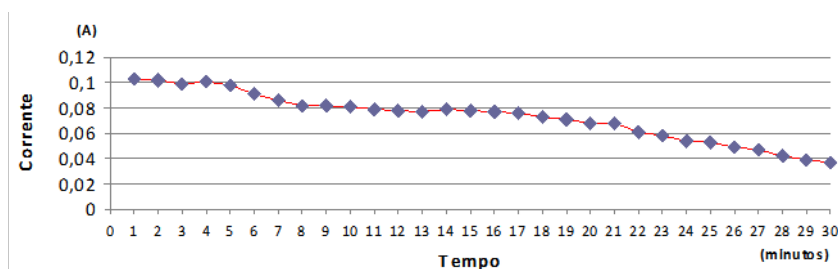
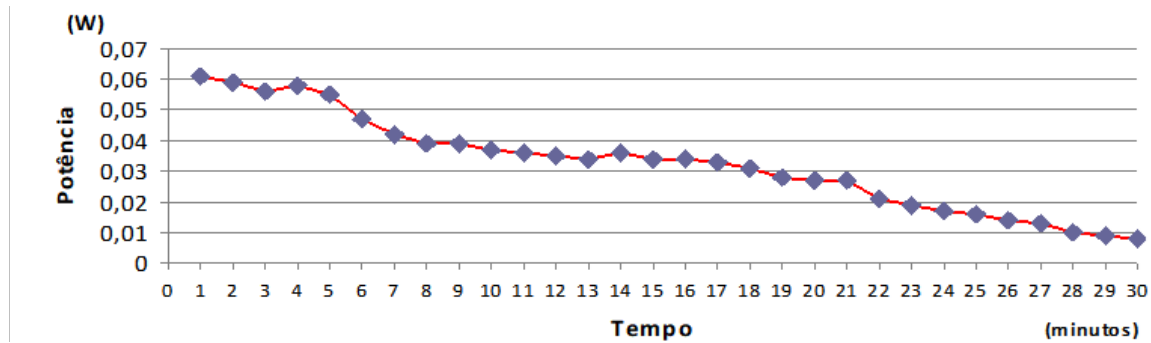


Figure 22 illustrates the reduction of the power output for a given load due to the reduction of  $\Delta t$  the thermoelectric module.

**Figure 22 - Measurement 1, power load of the thermoelectric module X test time**



The three graphs: voltage, current and power load demonstrate the immediate consequence of the uncontrolled increase of temperature on the cold side. All these graphs show reductions in their levels.

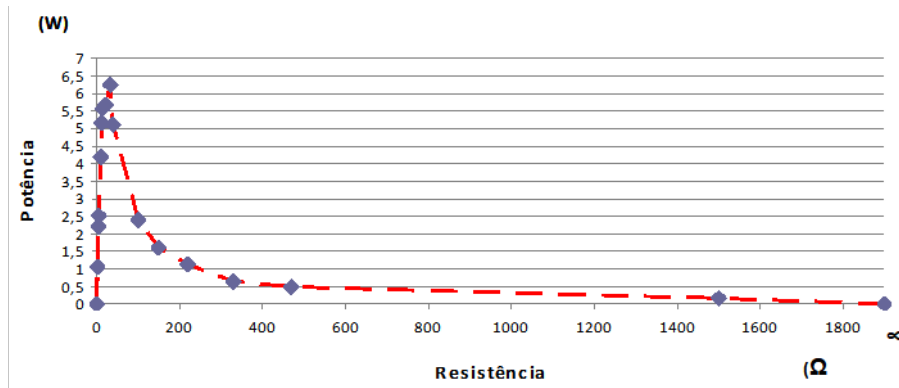
Thus it is proven the need for action on the variable - temperature of cold side (TF). Because of this, was used as a blanket of polyurethane thermal insulation to be used at points of care considered illustrated in Figure 26.

**Second Experimental Test (Measure 2).** After work on the problem identified in the measurement with a thermoelectric module, new measurements were performed. The start of measurement was performed after a stabilization period the temperature of hot and cold side of the thermoelectric module in order to observe the action of thermal insulation employed. A second measurement was also important for a better understanding of the influence of temperature on the photovoltaic module.

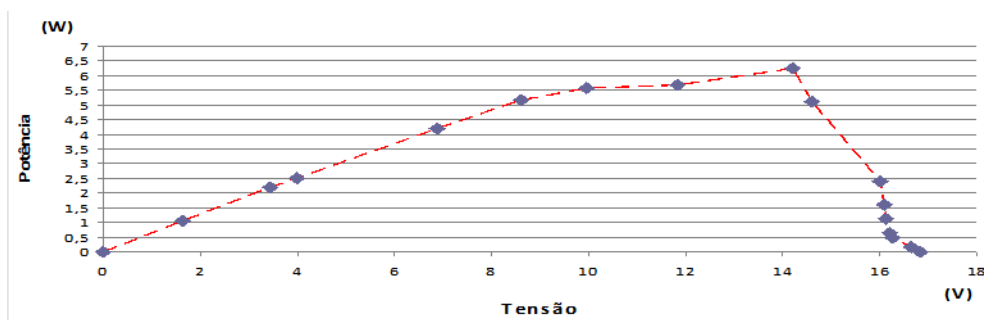
**Photovoltaic System - Measurement 2.** There was a clear reduction of power output compared to the data collected in a measurement which is a function of temperature increase of the system.

Figure 23 and Figure 24 illustrate, respectively, the power X resistênciade carga e a potênciade X the load voltage, it is observed compared to Figure 20 and Figure 22, one for measurement, a reduced power level in the load.

**Figure 23 - Measurement 2, power X load resistance of the photovoltaic system**

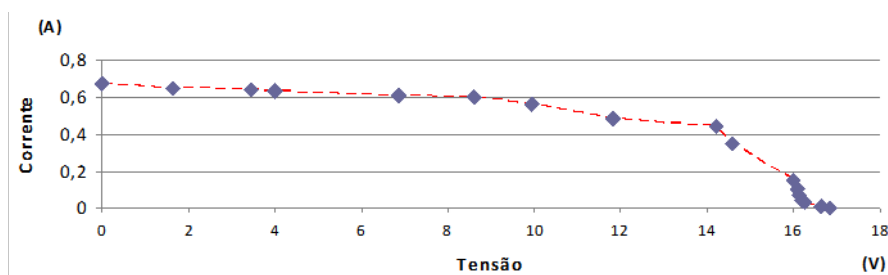


**Figure 24 - Measurement 2, power X the load voltage photovoltaic**



The characteristics of the photovoltaic module during the test measurement, as shown in Figure 25, have value of open circuit voltage reduced from the first measurement.

**Figure 25 - Measurement 2, current X the load voltage photovoltaic**



Under an overview Table 5 relating to the second measurement compared to Table 2 for a measurement, shows a reduction in the levels of output voltage and consequent reduction in the levels of output power with increasing temperature of the photovoltaic module.

**Thermoelectric System - Measurement 2.** After installation of thermal insulation for the treatment of the problem encountered as evidenced in Figure 26 of a measurement, new measurements were taken. Figure 26 illustrates the graph X  $\Delta t_t$  time test and demonstrates the stability of the variable. As  $\Delta t_t$  is the difference between the temperature of the hot side and cold

side of the thermoelectric module, Figure 26 also illustrates the behavior of variable temperature hot side and cold side. There is a stabilization in temperature of the cold side, that no one in the measurement, this breakthrough came in function of the installation of insulation at the point of attention described in Figure 26.

**Figure 26 - Measurement 2,  $\Delta t$  thermoelectric module X test time and temperature of the hot side and cold side of the thermoelectric module X test time**

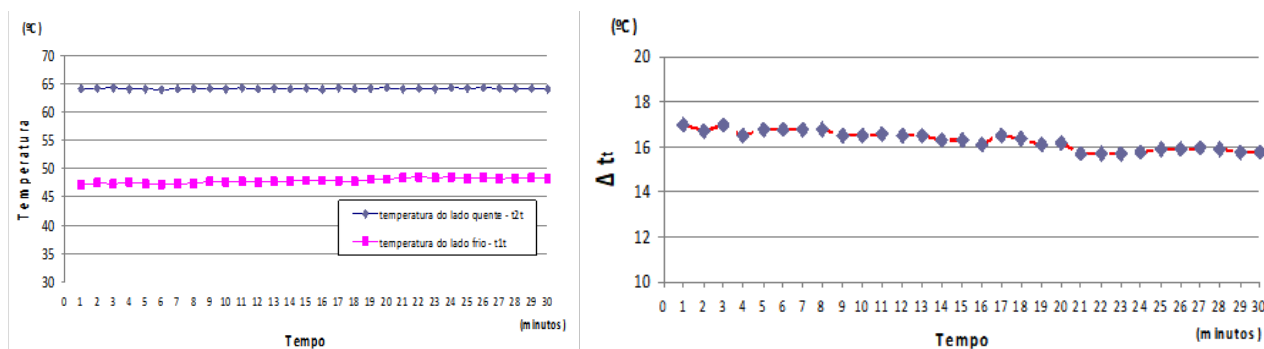
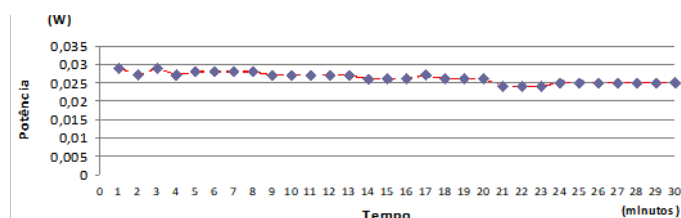


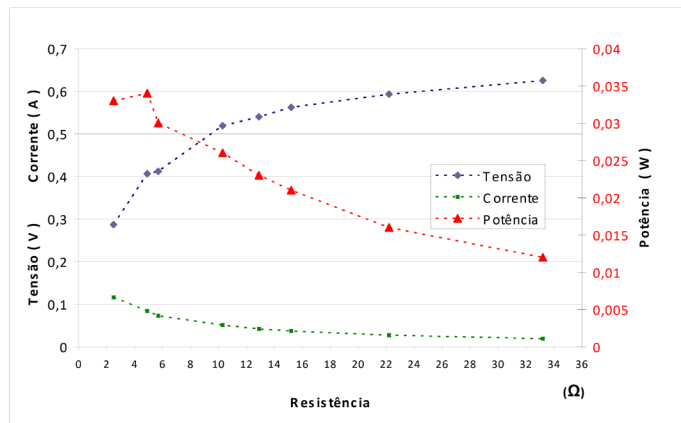
Figure 27 illustrates the power load X duration of the test, it was observed that the power has remained stable during the test. That did not happen in one measurement.

**Figure 27 - Measurement 2, power load of the thermoelectric module X test time**



As the second measurement was stable in relation to  $\Delta t$ , and thus have a greater stability in electricity generation. We conducted tests with a new variation of the load resistor in order to measure the voltage and current on the load and the power estimate. Figure 28 illustrates the behavior of current and voltage drop across the chart. With the increase of load resistance, there is an increase in tension and a decrease in load current, thus the product between the two that is the power in the load has a maximum point and is reduced as soon as at their level.

**Figure 28 - Measurement 2, voltage, current and power X load resistance of the thermoelectric module**



### COMPARISON BETWEEN SIMULATIONS AND TESTING

Photovoltaic System. Figure 29 illustrates the mathematical model to simulate the face of the measurements obtained in a test measurement, was considered to simulate a temperature approximately equal to the module found in the test concerning the first measurement, thereby the temperature of 54° C was used for simulation, it is possible to observe the similarity between a simulated current curve and the measuring points from the current test. The same applies to the curve of the simulated power compared to the calculated power points, which is nothing else than the product of the chain tension, both obtained in the assay.

**Figure 29 - Simulation and testing of photovoltaic system**

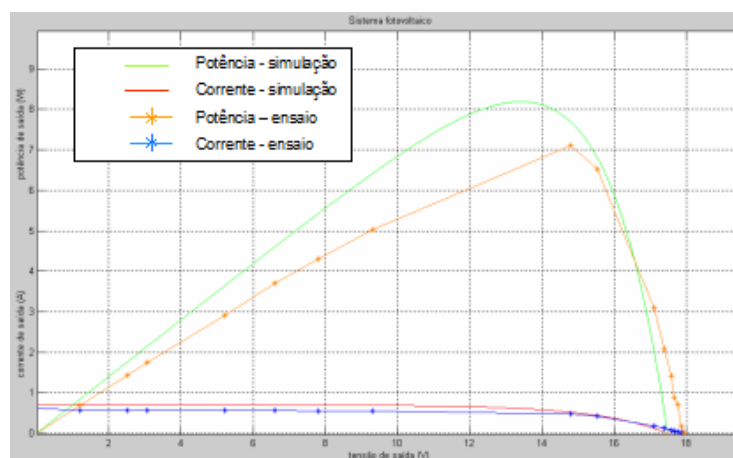
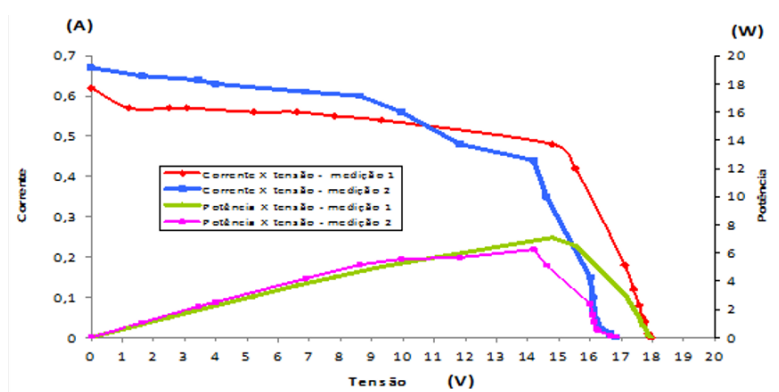


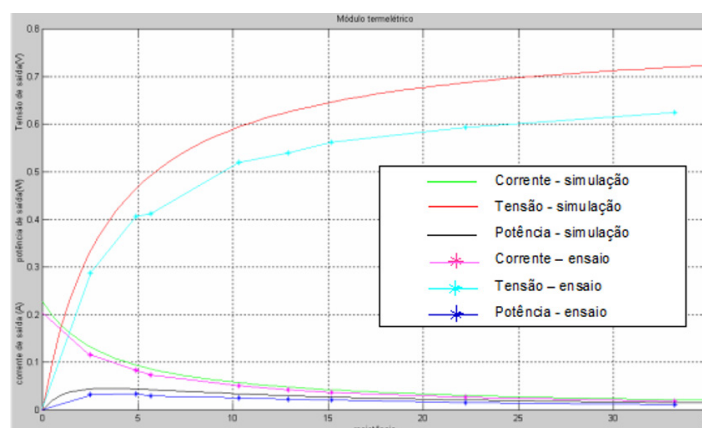
Figure 30 shows the results of measurements of first and second photovoltaic system. Clearly through graphics is possible to observe two important points: the maximum power achieved in the second measurement is less than the first measurement and the same applies to the open circuit voltage. Based on the theory presented can be assigned to these facts increase the temperature of the photovoltaic cell for measuring a second measurement, it appears that the average temperature during the test panel in a measurement was 54.3° C already when 2 measuring the average temperature was 64.1° C. Similar behavior was designed to simulate and illustrated by Figure 10.

**Figure 30 - Comparison between the measurements of the first and second photovoltaic module**



**Thermoelectric System.** Figure 31 illustrates the mathematical model to simulate the forward the measurements obtained in the tests, it is possible to observe the similarity between a voltage curve X simulated load resistance and the points measured during the test. The current has the same behavior as is observed graphically analyzing similarity between the curves and the simulated measurement points during the test. The power up because it represents the product of the two previous variables have similar behavior.

**Figure 31 - Simulation and testing of thermoelectric system**



## CONCLUSION

Through mathematical models presented in the study was possible to observe the influence of temperature on the systems. The simulations in MATLAB<sup>®</sup> 5.3 based on mathematical models have shown graphically presented the influence of temperature reduction in output voltage generated for the photovoltaic module, as for the thermoelectric module is possible to check the influence by temperature difference between hot and sides cold, where we observed a direct relationship between temperature difference and the tension generated by the Seebeck effect.

As the power load for both systems is a direct relationship with the tension generated, it was consequently influenced.

The results of the tests compared to the simulated results showed no significant deviation in this way has validated the use of mathematical models presented as a basis for analysis. During the tests it was observed the need to better control the temperature of the cold side, for the first test was not achieved a good stabilization of temperature, in the second test by analysis of the problem observed propagation of heat to the cold side of the thermoelectric module was achieved by a better stabilization after thermal insulation between the side panel photovoltaic and thermoelectric module.

In general, the goal was achieved because the heat which reduced the power delivered to a given load the photovoltaic system was used by the system for thermoelectric power generation. With the stabilization of the temperature of the cold side of the module using a thermal insulator, the temperature difference between hot and cold sides became more pronounced Seebeck effect thus generating more electricity. The thermoelectric module was used to improve the efficiency of the photovoltaic system and better use of the thermal energy from the Sun.

The thermoelectric module that was specified is used for cooling, although the same have behaved satisfactorily during tests, thus proving the reverse relationship between the Peltier and Seebeck effects, the theory shows that there is a difference between constructive models specified for cooling and thermoelectric power generation in this way for future trials suggest the use of thermoelectric modules specified for power generation.

After installation of thermal insulation between the sides of the thermoelectric and photovoltaic modules was observed on a better control of the temperature of the cold side, but

it was observed that the heat sink temperature rise is suffering through the heat exchange with the environment, thus influencing the raising the temperature of the cold side. It is necessary to effectively focus the heat dissipation system thermoelectric system.

## ACKNOWLEDGEMENTS

This work was financially supported by the Fellow Productivity and Technology Development in Innovative Extension/National Council for Scientific and Technological Development – CNPq, Brazil.

## LITERATURE REFERENCES

- C.V.T. Cabral, D.O. FILHO, L.V.B.M NETO, A.S.A.C. DINIZ, **Gerador fotovoltaico: Modelagem e simulação**. REVENG. Engenharia na agricultura. Viçosa. p. 262 – 268. (2009)
- E.O. Alves, Propriedades físicas do semicondutor Bi<sub>2</sub>Te<sub>3</sub>. Dissertação de Mestrado em física, Universidade federal do Rio Grande do Norte, Departamento de física teórica e experimental. Natal. 131p. (2007)
- J.R. Camargo; J.H. Santos; C.A. Chaves. Experimental performance of thermoelectric modules applied to power generation. 12<sup>th</sup> Brazilian Congress of Thermal Engineering and Sciences. Belo Horizonte. (2008)
- D.H.C. SOUZA. Otimização do uso de refrigeradores termoelétricos em processos de refrigeração. Brasília. (2007)
- A.M. Tonini and D.N. Schettino. Matlab para a engenharia. Centro Universitário de Belo Horizonte. Belo Horizonte. 50p. (2002)